HHS Public Access

Author manuscript

ACS Chem Neurosci. Author manuscript; available in PMC 2018 September 20.

Published in final edited form as:

ACS Chem Neurosci. 2017 September 20; 8(9): 1880–1888. doi:10.1021/acschemneuro.7b00022.

Ex vivo measurement of electrically evoked dopamine release in zebrafish whole brain

Mimi Shin, **Thomas M. Field**, **Chase S. Stucky**, **Mia N. Furgurson**, and **Michael A. Johnson**

Department of Chemistry, 1251 Wescoe Hall Drive, University of Kansas, Lawrence, KS 66045

Abstract

Zebrafish (*Danio rerio*) have recently emerged as useful model organism for the study of neuronal function. Here, fast-scan cyclic voltammetry at carbon-fiber microelectrodes (FSCV) was used to measure locally-evoked dopamine release and uptake in zebrafish whole brain preparations and results were compared with those obtained from brain slices. Evoked dopamine release ($[DA]_{max}$) was similar in whole brain and sagittal brain slice preparations (0.49 ± 0.13 μM in whole brain and 0.59 ± 0.28 μM in brain slices). Treatment with α-methyl-p-tyrosine methyl ester (αMPT), an inhibitor of tyrosine hydroxylase, diminished release and the electrochemical signal reappeared after subsequent drug washout. No observed change in stimulated release current occurred after treatment with desipramine or fluoxetine in the whole brain. Treatment with the uptake inhibitors nomifensine or GBR 12909 increased $[DA]_{max}$, while treatment with sulpiride, a D2 dopamine autoreceptor antagonist, resulted in increased stimulated dopamine release in whole brain, but had no effect on release in slices. Dopamine release in whole brains increased progressively up to an electrical stimulation frequency of 25 Hz, while release in slices increased up to a frequency of only 10 Hz and then plateaued, highlighting another key difference between these preparations. We observed a lag in peak dopamine release following stimulation, which we address using diffusion models and pharmacological treatments. Collectively, these results demonstrate the electrochemical determination of dopamine release in the whole, intact brain of a vertebrate species *ex vivo* and are an important step for carrying out further experiments in zebrafish.

Keywords

zebrafish; voltammetry; microelectrode; dopamine; release; autoreceptor

Introduction

Zebrafish (*Danio rerio*) are teleosts that were initially established as a model organism in the 1970s by George Streisinger for the study of development [1–3]. Recently, zebrafish have emerged as a desirable model for the study of neuronal function [4, 5] in part because they approximate the human central nervous system more accurately than invertebrates and are

Correspondence to: Michael A. Johnson.

Current address: Department of Chemistry, 1251 Wescoe Hall Drive, Lawrence, KS 66045

Author contributions: MS, TMF, and MAJ conceived of the experiments. MS, TMF, CSS, and MNF carried out the experiments. MS, TMF, and MAJ wrote the manuscript.

easier to genetically manipulate than rodents [6]. Moreover, the optical transparency of zebrafish larvae make this organism well-suited for *in vivo* studies in which intracellular calcium changes [7, 8] and action potentials [9] can be imaged real-time. Also, the zebrafish central nervous system, when studied using cultured cells [10], brain slices [11], and intact brain [12, 13], has proven amenable to electrophysiological measurements of neuronal firing.

In addition to these methods, the use of electrochemistry to measure the release and uptake of neurotransmitters in zebrafish is just now being realized. Fast-scan cyclic voltammetry at carbon-fiber electrodes (FSCV) is an electrochemical technique that provides good chemical selectivity and sub-second temporal resolution, allowing the measurement of the release and uptake of electroactive neurotransmitters[14–17]. FSCV has been used extensively in rodents to measure the release and uptake dynamics of dopamine, an abundant catecholamine neurotransmitter that plays a role in many aspects of neurological function, including the control of intentional movement[18, 19], cognition[20], and reward[21, 22].

Recently, the release of dopamine and other neurotransmitters was measured in sagittal brain slices acutely harvested from zebrafish, providing important proof of concept[23]. However, it is important to note that, although analysis of slices from various neuronal systems, especially rodents, have yielded much information regarding the study disease state mechanisms[24–28] as well as fundamental neurotransmitter release properties[29], brain slice preparations in general have several drawbacks, such as cellular damage induced at the surface of the slice[30–32] and difficulty in capturing entire neuronal pathways[33, 34]. The use of intact brains could mitigate these problems by decreasing the amount of tissue damage and leaving the neuronal pathways intact, thereby allowing remote stimulation of the pathway and eliminating the release of interfering neurotransmitters and neuromodulators that would be present upon local stimulation. Additionally, constant potential amperometry has recently been used to measure stimulus evoked dopamine release in zebrafish larvae[35]. However, to our knowledge, FSCV measurements of neurotransmitter release within the intact brains of adult zebrafish have not yet been reported in the literature; thus, the measurement of locally-stimulated dopamine release from acutely harvested, intact zebrafish brains, and comparison of these measurements with those from brain slices, represents a critical first step.

Here, we describe measurements of dopamine release and uptake in whole, intact zebrafish brains with FSCV. Furthermore, we compare these measurements to those obtained in sagittal and coronal brain slices. We found that, when the working electrode is properly placed by reference to the external features of the removed brain, electrically evoked dopamine release and uptake is easily measured in zebrafish whole brain *ex vivo*. The cyclic voltammograms (CV) obtained suggest that the primary neurotransmitter measured is dopamine. Moreover, we confirmed the presence of dopamine with pharmacological agents that alter dopamine release and uptake. Some of the unique characteristics of release and uptake curves are also discussed. These results support the use of FSCV in *ex vivo* whole brain preparations as a useful analytical tool for measuring neurotransmitter release and uptake in zebrafish.

Results and Discussion

Evoked dopamine release in zebrafish

A photograph of a viable whole brain acutely harvested from an adult zebrafish is shown in Fig. 1A. The brain is situated ventral side face up to provide easier access to the subpallium in the telencephalon, a region of the brain that contains dopaminergic innervation[36–38]. The carbon-fiber microelectrode and the stimulation electrodes were manipulated into place by referencing the external features of the ventral side of the brain. The carbon-fiber microelectrode was positioned 100 μm laterally from the medial olfactory tract (MOT) and inserted 280–300 μm deep. The region was stimulated locally with a biphasic stimulus pulse regimen in which 25 pulses, 2 ms duration and 350 μA current, was applied. Application of this regimen resulted in the release of dopamine detected by FSCV (Fig. 1C). A stimulated release plot (concentration versus time profile), sampled from the color plot at the horizontal dotted line, is located above the color plot. A cyclic voltammogram (CV), sampled at the vertical dashed line of the color plot, serves as electrochemical evidence that the neurotransmitter released is dopamine.

In order to determine how spatially resolved our method is we kept the stimulation electrode stationary and moved the working electrode inferior and superior from the MOT as well as dorsally. We found that as the electrode was moved away from the MOT both superior and inferior the release event was no longer observed. These results suggest that the region that is dopamine rich is specific (Supplementary Data, Fig. 1).

For comparison, dopamine release was also measured in acutely harvested sagittal brain slices (Figs. 1B and D). The stimulation and working electrodes were positioned at the ventral telencephalon and release was evoked locally using the same stimulation parameters used in the whole brain. Both CV and stimulated release plots are similar to those obtained in the whole brain preparation. In the representative raw data, $[DA]_{max}$ increased until a peak concentration of about 0.5 μM was reached ~2 s after stimulus application. Current then decreased as uptake occurred. Observation of the color plots suggest that other electroactive species were not released in substantial quantities. Also, electrically evoked $[DA]_{max}$ was consistent throughout each recording session. Dopamine release measurements in both preparations were collected for one hour and compared.

Data pooled from multiple whole brains and brain slices reveal that, under equivalent stimulation conditions, average $[DA]_{max}$ was not significantly different in whole brain and slices: 0.41 ± 0.07 μM in whole brains and 0.54 ± 0.13 μM in slices ($p = 0.40$, n=9 slices and 9 brains, t-test). The concentration of dopamine release evoked by either single or multiple stimulus pulses, both *in vivo* and *ex vivo*, has been reported extensively in the literature. For example, application of single pulses in mouse brain slices resulted in $[DA]_{max}$ values of 1.43 ± 0.11 μM (striatum) [39], 1.42 ± 0.14 μM (nucleus accumbens core), and 1.40 ± 0.19 μM (caudate putamen) [40]. Multiple stimulation pulses were applied *in vivo* to evoke dopamine release in the rat striatum at a reported peak concentration of 1.04 ± 0.14 μM[41]. Recently, Jones et al.[23] found dopamine to be released in zebrafish sagittal slices at a peak concentration of about 100 nM following stimulation with 20, 4-ms duration pulses applied at a current of 500 μA and an application frequency of 60 Hz. In any case, it appears from

our results that less dopamine is released in zebrafish whole brain and slices compared to that of rodents.

Effect of pharmacological agents on evoked dopamine release

Extracellular dopamine levels are tightly regulated by the dopamine transporter (DAT), a membrane-bound protein that transfers dopamine molecules from the extracellular space to the intracellular space within neurons[42]. The stimulated release plot reveals that, similar to the mammalian brain, dopamine is immediately taken up after release. Based on previous measurements in brain slices from mice that lack the DAT [43, 44], it is likely that dopamine is actively taken up and that the decrease in current is not a result of diffusion away from the electrode.

Additional pharmacological studies were conducted in which whole brain preparations, along with sagittal and coronal slices, were treated with 10 μM nomifensine (Fig. 2), a well-established dopamine uptake inhibitor[42]. As a result, the rate of dopamine uptake was sharply diminished, indicated by the decreased slope of the stimulated release curves after peak dopamine release. This treatment resulted in a ~130% increase in $[DA]_{max}$ in the whole brain preparation (Fig. 2A: pre-drug, 0.34 ± 0.14 μM; post-drug, 0.79 ± 0.22 μM, $p < 0.05$, n = 4 brains, t-test). A similar effect was observed in sagittal slices, with $[DA]_{max}$ increasing ~100% (Fig. 2B: pre-drug, 0.49 ± 0.13 μM; post-drug, 0.97 ± 0.18 μM, $p < 0.05$, n = 5 slices, t-test) and in coronal slices, increasing ~100 % (Fig 2C: pre-drug 0.42 ± 0.11 μM ; post-drug, 0.82 ± 0.13 μM, $p < 0.05$, n = 4 slices, t-test). Our measurements also revealed a nearly complete attenuation of uptake in all three preparations treated with nomifensine (Fig 2A, B, and C). Release plots obtained after treatment with nomifensine concentrations ranging from 1 to 1000 nM (Fig. 3A) failed to reveal a statistically significant effect on $[DA]_{max}$ (one-way ANOVA, $p = 0.11$, n=3 brains)(Fig. 3B); thus, it appears that nomifensine substantially affects $[DA]_{max}$ only at higher drug concentrations.

In order to compare relative signal contributions from dopamine with those from norepinephrine and serotonin, two other common biogenic amine neurotransmitters, 10 μM GBR-12909, a selective dopamine uptake inhibitor, 10 μM desipramine[45], a selective norepinephrine uptake inhibitor, and 10 μM fluoxetine[46], a selective serotonin uptake inhibitor, were perfused over *ex vivo* whole brain preparations (Figs 4A, B, and C). GBR-12909 treatment resulted in a significant increase in peak amplitude, similar to the findings of Jones *et al.* (Figs. 4A and D; $p< 0.05$, t-test, n = 5). However, treatment with desipramine and fluoxetine resulted in no statistically significant change in $[DA]_{max}$ (Figs. 4B, C, and D; desipramine pre-drug 0.43 ± 0.08 μM; post-drug 0.50 ± 0.09 μM; $p = 0.60$, n= 5 brains, t-test and fluoxetine pre-drug 0.27 ± 0.05 μM, post-drug 0.33 ± 0.04 μM $p = 0.35$, n= 5 brains, t-test). Dopamine transporters clearly play a role in determining the magnitude of the signal, while norepinephrine and serotonin transporters do not. Thus, these results confirm the presence of dopamine and infer the absence of norepinephrine and serotonin. Further evidence that serotonin is not present is provided by the difference in the shape of its CV from that of dopamine [47].

To obtain additional confirmation of neurotransmitter identity, we examined the effect of α-methyl-p-tyrosine methyl ester (αMPT), which inhibits tyrosine hydroxylase and blocks

monoamine neurotransmitter synthesis (Fig. 5A). Release was electrically-evoked and measured every 10 minutes. Upon stabilization of the dopamine signal, brains were perfused with 50 μM αMPT and, approximately 2 hours later, the observed signal was greatly diminished (pre-drug, 0.56 ± 0.08 μM; post-drug, 0.14 ± 0.07 μM, $p < 0.005$, one-way ANOVA). To ensure that this disappearance of release was not due simply to loss of neuronal viability, the drug was washed out, and release re-appeared approximately 1 hour later (washout, 0.51 ± 0.10 μM, $p = 0.40$, one-way ANOVA), indicating that neurotransmitter release was not significantly different than before the drug was added (Fig. 5B). These measurements, taken in conjunction with the uptake inhibition experiments, further indicate that the neurotransmitter detected is a catecholamine, and suggest that other classes of electroactive neurotransmitters, such as serotonin and histamine, are not released.

Based on the following results, described in this work and in work by others, we conclude that dopamine is the major contributor to the observed signal. First, the peak current observed following stimulation is unaffected by treatment with 10 μM desipramine (Fig. 4), yet is increased by treatment with 10 μM nomifensine (Fig. 2) and 10 μM GBR-12909 (Fig. 4). Given that the inhibition constants (K_i) are likely in the low nM range for nomifensine at the dopamine and norepinephrine transporters[48] and also for desipramine at the norepinephrine transporter[49], dopamine and norepinephrine uptake should be almost completely inhibited based on the concentrations used. Thus, differences in measured peak current between these two drug treatments would reflect differences in release between dopamine and norepinephrine since diffusion alone is insufficient to substantially decrease measured extracellular levels on the timescale of our measurements (20 s)[50]. Second, anatomical data obtained from morpholino knockdown experiments in zebrafish larvae suggest that tyrosine hydroxylase-expressing neurons projecting into the forebrain are mostly dopaminergic[51]. Finally, work by Shang et al.[52] suggests that dopamine is the primary catecholamine released in this brain region. Clearly, more work needs to be done to quantify the relative amounts of dopamine, norepinephrine, and other neurotransmitters released in the telencephalon and other brain regions. However, we can conclude from this work that extracellular dopamine levels are tightly regulated by DAT in the telencephalon immediately after release and that *ex vivo* whole brain preparations can be used to measure locally-stimulated dopamine release.

Dopaminergic terminals in the mammalian striatum possess D2-family dopamine autoreceptors that serve as a regulatory feedback mechanism for dopamine release[42]. To determine if a similar self-regulatory mechanism is present in dopaminergic terminals of the subpallium, we perfused whole brain *ex vivo* preparations with 10 μM sulpiride, a D2-family dopamine receptor inhibitor (Fig. 6A). Approximately 1 hour after addition of drug, dopamine release increased by about 80% (pre-drug, 0.41 ± 0.12 μM; post-drug, 0.74 ± 0.13 μM, $p < 0.05$, t-test). Thus, D2 receptors are also present in the zebrafish brain and appear to serve a similar regulatory function. However, given that the circuitry is still intact in the whole brain preparation, it is also possible that sulpiride may enhance the release of dopamine by antagonism of dopamine receptors located not only presynaptically, but also at other locations within the brain[53].

To determine if autoregulation by D2 receptors occurs specifically at terminals, electrically-evoked dopamine release was measured in the subpallium of sagittal (Fig. 6B) and coronal (Fig. 6C) brain slices before and after sulpiride treatment. The slicing process could at least partially disrupt the ascending dopaminergic pathway from the diencephalon to the subpallium, leaving only presynaptic terminals without dopaminergic soma [36, 37]. In sagittal slices, $[DA]_{max}$ appeared to increase upon drug treatment, but this increase was not statistically significant (pre-drug, 0.33 ± 0.12 μM; post-drug, 0.68 ± 0.29 μM, p = 0.13, n = 5 fish, t-test)(Fig. 6D). Additionally, $[DA]_{max}$ also did not increase in coronal slice preparations (pre-drug, 0.35 ± 0.12 μM; post-drug, 0.38 ± 0.10 μM, p = 0.47, n = 5 fish, t-test). Our results suggest that, while there is an effect on D2 receptors in whole brains, this effect is disrupted in slice preparations. The reason for this lack of effect in zebrafish is not well-understood; however, it is possible that the D2 receptors are not located presynaptically, but rather on the soma[53]. Given that D2 receptors are also found on the cell bodies and axon in rodents, this arrangement would not be unprecedented in zebrafish[54]. Another possibility is that the slicing process induces damage to the terminals. Additional studies will be required to identify the underlying mechanisms of this phenomenon.

Kinetics of neurotransmitter release and uptake

The dopamine release curves in zebrafish whole brain preparations have several interesting characteristics: (1) the curves have a tendency to not return to baseline levels after the release event ('hang-up', see Supplementary Fig. 2), (2) $[DA]_{max}$ is observed to occur a certain amount of time after the end of the electrical stimulation, a phenomenon known as overshoot (Δt_O), and (3) dopamine release sometimes appears to occur a very short time after electrical stimulation is initiated, a phenomenon known as lag (Δt_L). Figure 7A illustrates the concepts of overshoot and lag.

In addressing the first point, it was observed from the αMPT measurements that, after application of the inhibitor, the signal observed after the release event was greatly diminished (Fig. 5). This phenomenon points to the hang-up being related to the dopamine initially released and not some secondary release event. A plausible explanation is that the signal represents dopamine adsorbed to the surface of the carbon-fiber microelectrode. This phenomenon has been described previously when measuring dopamine release in rats[55].

In addressing points (2) and (3), it is important to note that overshoot and lag are phenomena also observed in rodents both *in vivo* and *ex vivo* [56]. The concepts of overshoot and lag are explained by the tendency for released dopamine to diffuse from synapse to the electrode; thus, we hypothesize that the time needed for this diffusion leads to Δt_O and Δt_L (Fig 7A) [57, 58]. In order to examine the possible relationship between diffusion and Δt_O and Δt_L in zebrafish whole brain, the stimulation frequency was varied from 10 to 60 Hz while other stimulation parameters were held constant (120 pulses, 350 μA, 4 ms). If simple diffusion is all that is involved, it would be expected that Δt_O and Δt_L would be similar in magnitude and would remain constant while stimulation parameters change[57, 59]. This is because in the so called diffusion gap model (Equation 1), diffusion is assumed to be independent of any variable except the distance between the electrode (represented by x) and site of release.

$$\frac{d[DA]}{dt} = D\frac{\partial^2[DA]}{\partial x^2} + [DA]_p f - \frac{V_{\max}[DA]}{[DA] + K_M} \quad \text{(Equation 1)}$$

In this equation, V_{max} and K_M are the Michaelis–Menten parameters, f is stimulation frequency, [DA] is the concentration of dopamine at any given point in time, $[DA]_p$ is the amount of dopamine release per electrical stimulus pulse, a parameter that is corrected for uptake and electrode performance [60], and D is the diffusion coefficient of dopamine. The first term on the right side is from Fick's Second Law[61, 62] and accounts for diffusion of dopamine to the electrode, the second term accounts for the total amount of dopamine released, and the third term accounts for dopamine uptake[60]

When the model is applied, a gap width is used that represents the distance between the electrode and the point of release[57]. As this gap increases, the lag and overshoot should increase by approximately equal amounts. On the other hand, if the gap remains the same the lag and overshoot should be approximately constant. We observed that, as the stimulation frequency was increased and the electrode was held in place, both concentration and Δt_O increased in a linear fashion (slope ≠ 0, $p < 0.05$, $R^2 = 0.73$; slope ≠ 0 $p < 0.005$, $R^2 = 0.908$ respectively, Figs. 7B and C). As $[DA]_{max}$ is increasing, Δt_O is also increasing. This result directly contradicts the prediction of the diffusion gap model that Δt_O should remain constant[57]. It is also important to note that, in the vast majority of traces, we did not observe a Δt_L greater than the 100 ms temporal resolution of our method (data not shown), which also points to the diffusion gap model as not holding; therefore, another model must be considered.

This phenomenon of Δt_O being present and independent of Δt_L, and sensitive to the change in stimulation parameters, has been observed by Taylor *et al.* [63] in rats treated with nomifensine. In particular, as dopamine concentration increased due to inhibition of DAT, Δt_O also increased while Δt_L was nonexistent. They explained this phenomenon through a restricted diffusion model[57]. Briefly, this model assumes that dopamine needs to diffuse to the electrode through tissue, so that that diffusion will not be unhindered, but rather will be interfered with by various characteristics of the tissue such as tortuosity[64] or absorption to specific sites in the tissue[65]. During a release event in the absence of drug, reuptake is much faster than the restricted diffusion so the dopamine that is restricted gets uptaken before it has a chance to move to the electrode, resulting in a small or nonexistent Δt_O. However, after nomifensine treatment, since uptake is significantly slowed, the restricted dopamine molecules are able to diffuse to the electrode for a relatively long time and Δt_O becomes large.

In zebrafish, it is unclear what the amplitude of a naturally occurring transient is; however, we propose that, in the case of stimulated release, the amount of dopamine released is so great that DAT becomes saturated. This saturation causes dopamine to remain in the tissue for a long period of time. During this time, it can diffuse, resulting in the large Δt_O we observe. More experiments are needed to verify this hypothesis; however, our data clearly

show that, in zebrafish, the issue of diffusion and its role in regulation of dopamine concentration is complex.

Effect of stimulation frequency on evoked dopamine release

The degree of dopamine release is determined, in part, by the number of stimulus pulses and the frequency (number of biphasic pulses applied per second)[66]. Initially, to determine if alteration of stimulation frequency impacts dopamine release similarly in zebrafish, evoked dopamine both in whole brain and sagittal slices was measured and compared at frequencies ranging from 5 Hz to 25 Hz while other stimulus parameters were held constant (120 pulses, 4 ms, and 350 μA; Fig. 8).

We found a trend of increasing dopamine release up to a frequency of 25 Hz in whole brain. Although there appears to be a slight curvature, linear regression analysis revealed a strong correlation coefficient of linearity (R^2=0.96) and also a significantly non-zero slope ($p = 0.003$). In slices, dopamine release increased at 10 Hz; however, beyond 10 Hz, the curve plateaued (R^2=0.17). The overall slope of this curve did not significantly deviate from zero ($p = 0.49$). The difference in curves may suggest that the preparation impacts the availability of vesicles for release. Previously, progressively diminishing increases of dopamine release [28] had been observed in rodent brain slices and linear increases had been observed *in vivo* [67] when stimulation frequency was increased. While the causes underlying these differences are not known, it is possible that higher stimulation frequencies result in mobilization of reserve pool vesicles, as our previous results in striatal mouse brain slices have suggested [28]. In fact, this decrease in release at higher frequencies was exaggerated in transgenic R6/2 mice, which are commonly used to model Huntington's disease (HD). Our previous results have suggested that this decrease is likely due to a diminished reserve pool in R6/2 mice. In the future, it will be interesting to determine if these differences between slices and whole brain arise from a diminished reserve pool or have some other cause.

Conclusion

We have shown that dopamine release can be easily measured with FSCV in the subpallium of zebrafish whole brain. This preparation offers the advantage of keeping the whole brain intact, thereby preserving the three-dimensional neuronal circuitry and offering the future possibility of measuring release evoked by stimulation of pathways. Similar to slices, extracellular dopamine levels are tightly regulated by uptake through the DAT. Our results also demonstrate that uptake is inhibited by nomifensine in both brain slice and whole brain preparations.

Importantly, in their recent paper, Jones *et al.* showed that evoked neurotransmitter release could be easily measured in slices[23]. Our work has not only built upon these findings, but it has also revealed other release characteristics that are apparently not found in zebrafish sagittal slice preparations. We have identified important differences between slices (sagittal and coronal) and whole brain. For example, even though D2 autoreceptors regulate dopamine release in whole brain and sagittal slice preparations, similar to that observed in rodents, D2 antagonism has no effect in slices. Moreover, stimulated release in sagittal slices responded differently to increasing stimulation frequency compared to release in whole

brain. Finally, stimulated release plots in the whole brain preparation had interesting features, including a tendency to not return to baseline following the stimulated release of dopamine and a propensity for dopamine release to continue even after the end of the electrical stimulus. It is apparent that these processes reflect complexities in zebrafish neuronal function that must be sorted out with additional studies. Moreover, our studies reveal not only that release measurements in whole brain is a viable option that may be of particular use in studying circuit function, but also that there are differences between whole brain, coronal slices, and sagittal slices that should be addressed before moving forward.

In summary, these results represent an important step toward more complex studies, such as FSCV experiments that make use of remote stimulation in zebrafish whole brain and measurements of dopamine release *in vivo*. Furthermore, the expanded use of this model organism will allow researchers to exploit the genetic advantages of zebrafish in the analysis of neurotransmitter release properties.

Methods

Chemicals

Dopamine, α-methyl-p-tyrosine methyl ester (αMPT), nomifensine, and (±) sulpride, were purchased from Sigma-Aldrich (St. Louis, MO). All aqueous solutions were made with purified (18.2 MΩ) water. A modified artificial cerebrospinal fluid (aCSF) for zebrafish consisted of 131 mM NaCl, 2mM KCl, 1.25 mM KH_2PO_4, 20 mM $NaHCO_3$, 2mM $MgSO_4$, 10 mM glucose, 2.5 mM $CaCl_2{\cdot}H_2O$, and 10mM HEPES, and the pH was adjusted to 7.4. Dopamine stock solutions were prepared in 0.2 M perchloric acid and were diluted with aCSF without glucose for calibrations. Solutions of 50 μM aMPT, 10 μM nomifensine, and 10 μM sulpride, were prepared the day of each experiment.

Electrochemical Measurements

Cylindrical carbon-fiber microelectrodes were fabricated as previously described. Briefly, 7 μm diameter carbon fibers (Goodfellow Cambridge LTD, Huntingdon, UK) were aspirated into glass capillary tubes (1.2 mm D.D and 0.68 mm I.D, 4 in long; A-M Systems, Inc, Carlsborg, WA, USA). Loaded capillaries were then pulled using a PE-22 heated coil puller (Narishige Int. USA, East Meadow, NY) and carbon fibers were trimmed to a length of 30 μm from the pulled glass tip. To seal the carbon fibers, electrodes were dipped into epoxy resin (EPON resin 815C and EPIKURE 3234 curing agent, Miller-Stephenson, Danbury, CT, USA) and cured at 100 °C for 1 hour. The electrodes were soaked in isopropanol for 10 minutes, and the electrode surface was electrochemically pretreated by scanning with the waveform –0.4 V to +1.3 V back to –0.4 V at a frequency of 60 Hz for 15 min followed by 10 Hz for 10 min. Electrodes were then backfilled with 0.5 M potassium acetate for electrical connection. A chlorided Ag wire was used as the Ag/AgCl reference electrode. Data were collected and analyzed using an electrochemical workstation consisting of a Dagan Chem-Clamp potentiostat (Dagan, Minneapolis, MN, USA), modified to allow decreased gain settings, a personal computer with Tar Heel CV software (provided by R.M. Wightman, University of North Carolina, Chapel Hill, NC, USA.), a UEI breakout box (UNC chemistry department electronics design facility, Chapel Hills, NC), and two National

Instruments computer interface cards (PCI 6052 and PCI 6711, National Instruments, Austin, TX). The waveform was applied every 100 ms to the electrode at a scan rate of 400 V/s. Electrodes were calibrated with a 1 μM dopamine solution. To evoke dopamine release both in whole brain and brain slices, multiple stimulus pulses (25 pulses, 2 ms, 350 μA) was applied for 0.5 s at 5 s unless mentioned otherwise. This stimulation was applied by two tungsten electrodes 200 μm apart. A recovery time of 10 min between stimulations was used for both whole brain and brain slices experiments.

Zebrafish

All animal procedures were approved by the University of Kansas Institutional Animal Care and Use Committee. Zebrafish were housed in the Molecular Probes Core of the Center for Molecular Analysis of Disease Pathways at the University of Kansas. Zebrafish were euthanized by rapid chilling, and then decapitated. Brains were harvested under a dissection stereoscope (Leica Microsystem, Bannockburn, IL, USA) and transferred to a superfusion chamber in which they were kept viable by continuous flow of oxygenated (95% O_2 and 5% CO_2) aCSF maintained at a temperature of 28ºC. The brain was immobilized by placement of a nylon mesh harp on top. Brains were allowed to equilibrate in the chamber for 1 hour prior to collecting measurements. For brain slice preparation, harvested brains were suspended in 2% low gelling point agarose (agarose type VII-A, Sigma-Aldrich, St Louis, MO, USA) prepared in 50% distilled water and 50% aCSF. After hardening, a block of agarose containing the brain was cut off and glued onto a specimen disk and fastened in the buffer tray of a vibratome (Leica Microsystem, Bannockburn, IL, USA). The tray was filled with ice cold oxygenated aCSF and kept at 2–4°C during slicing. Sagittal and coronal slices, 350 μm thick, were transferred to the perfusion chamber and were allowed to equilibrate for 1 hour prior to collecting measurements.

Statistical Analysis

Statistical analyses were accomplished using Graph Pad Prism 6 (Graph Pad Software, Inc., La Jolla, CA, USA). All data are reported as a mean plus or minus the standard error of the mean.

Supplementary Material

Refer to Web version on PubMed Central for supplementary material.

Acknowledgments

This research was funded by the Center for Molecular Analysis if Disease Pathways (CMADP) at the University of Kansas (P20 GM103638), an NIH Center of Biomedical Research Excellence. Additional support was provided by the Molecular Probes Core facility of the CMADP. Funding was also provided by the University of Kansas. The authors thank Prof. Blake Peterson, University of Kansas, and Prof. Lesa R. Hoffman, University of Kansas, for technical assistance.

Abbreviations

FSCV	fast-scan cyclic voltammetry
αMPT	α-methyl-p-tyrosine methyl ester

DAT	dopamine transporter
CV	cyclic voltammogram
$[DA]_{max}$	peak dopamine concentration

References

1. Grunwald DJ, Eisen JS. Headwaters of the zebrafish -- emergence of a new model vertebrate. Nat Rev Genet. 2002; 3:717–724. [PubMed: 12209146]
2. Williams R. Thanks be to zebrafish. Circ Res. 2010; 107:570–572. [PubMed: 20814025]
3. Li, H-h, Huang, P., Dong, W., Zhu, Z-y, Liu, D. A brief history of zebrafish research-toward biomedicine. Yichuan. 2013; 35:410–420.
4. Friedrich RW, Jacobson GA, Zhu P. Circuit Neuroscience in Zebrafish. Curr Biol. 2010; 20:R371–R381. [PubMed: 21749961]
5. Fetcho JR, Liu KS. Zebrafish as a Model System for Studying Neuronal Circuits and Behaviora. Annals of the New York Academy of Sciences. 1998; 860:333–345. [PubMed: 9928323]
6. Kimmel CB, Ballard WW, Kimmel SR, Ullmann B, Schilling TF. Stages of embryonic development of the zebrafish. Developmental dynamics : an official publication of the American Association of Anatomists. 1995; 203:253–310. [PubMed: 8589427]
7. Ahrens MB, Li JM, Orger MB, Robson DN, Schier AF, Engert F, Portugues R. Brain-wide neuronal dynamics during motor adaptation in zebrafish. Nature. 2012; 485:471–477. [PubMed: 22622571]
8. Higashijima, S-i, Masino, MA., Mandel, G., Fetcho, JR. Imaging neuronal activity during zebrafish behavior with a genetically encoded calcium indicator. J Neurophysiol. 2003; 90:3986–3997. [PubMed: 12930818]
9. Randlett O, Wee CL, Naumann EA, Nnaemeka O, Schoppik D, Fitzgerald JE, Portugues R, Lacoste AM, Riegler C, Engert F. Whole-brain activity mapping onto a zebrafish brain atlas. Nature Methods. 2015; 12:1039–1046. [PubMed: 26778924]
10. Qin Z, Lewis J, Perry S. Zebrafish (Danio rerio) gill neuroepithelial cells are sensitive chemoreceptors for environmental CO2. The Journal of physiology. 2010; 588:861–872. [PubMed: 20051495]
11. Rothenaigner I, Krecsmarik M, Hayes JA, Bahn B, Lepier A, Fortin G, Götz M, Jagasia R, Bally-Cuif L. Clonal analysis by distinct viral vectors identifies bona fide neural stem cells in the adult zebrafish telencephalon and characterizes their division properties and fate. Development. 2011; 138:1459–1469. [PubMed: 21367818]
12. Baraban S, Taylor M, Castro P, Baier H. Pentylenetetrazole induced changes in zebrafish behavior, neural activity and c-fos expression. Neuroscience. 2005; 131:759–768. [PubMed: 15730879]
13. Baraban SC. Forebrain electrophysiological recording in larval zebrafish. J Vis Exp. 2013
14. Venton BJ, Wightman RM. Psychoanalytical electrochemistry: dopamine and behavior. Analytical Chemistry. 2003; 75:414 A–421 A.
15. Hermans A, Keithley RB, Kita JM, Sombers LA, Wightman RM. Dopamine detection with fast-scan cyclic voltammetry used with analog background subtraction. Analytical chemistry. 2008; 80:4040–4048. [PubMed: 18433146]
16. Wightman RM. Probing cellular chemistry in biological systems with microelectrodes. Science. 2006; 311:1570–1574. [PubMed: 16543451]
17. Robinson DL, Hermans A, Seipel AT, Wightman RM. Monitoring rapid chemical communication in the brain. Chemical reviews. 2008; 108:2554–2584. [PubMed: 18576692]
18. Barnéoud P, Descombris E, Aubin N, Abrous DN. Evaluation of simple and complex sensorimotor behaviours in rats with a partial lesion of the dopaminergic nigrostriatal system. European Journal of Neuroscience. 2000; 12:322–336. [PubMed: 10651887]
19. Cousins M, Salamone J. Involvement of ventrolateral striatal dopamine in movement initiation and execution: a microdialysis and behavioral investigation. Neuroscience. 1996; 70:849–859. [PubMed: 8848171]

20. Aarts E, van Holstein M, Cools R. Striatal dopamine and the interface between motivation and cognition. Frontiers in psychology. 2011; 2
21. Kelley AE, Berridge KC. The neuroscience of natural rewards: relevance to addictive drugs. The Journal of neuroscience. 2002; 22:3306–3311. [PubMed: 11978804]
22. Oei NY, Rombouts SA, Soeter RP, van Gerven JM, Both S. Dopamine modulates reward system activity during subconscious processing of sexual stimuli. Neuropsychopharmacology. 2012; 37:1729–1737. [PubMed: 22395731]
23. Jones LJ, McCutcheon JE, Young AM, Norton WH. Neurochemical measurements in the zebrafish brain. Frontiers in behavioral neuroscience. 2015; 9
24. Good CH, Hoffman AF, Hoffer BJ, Chefer VI, Shippenberg TS, Bäckman CM, Larsson N-G, Olson L, Gellhaar S, Galter D. Impaired nigrostriatal function precedes behavioral deficits in a genetic mitochondrial model of Parkinson's disease. The Faseb Journal. 2011; 25:1333–1344. [PubMed: 21233488]
25. Zhang L, Le W, Xie W, Dani JA. Age-related changes in dopamine signaling in Nurr1 deficient mice as a model of Parkinson's disease. Neurobiol Aging. 2012; 33:1001.e1007–1001.e1016.
26. Robertson GS, Robertson HA. Evidence that L-dopa-induced rotational behavior is dependent on both striatal and nigral mechanisms. J Neurosci. 1989; 9:3326–3331. [PubMed: 2795165]
27. Covey DP, Garris PA. Using fast-scan cyclic voltammetry to evaluate striatal dopamine release elicited by subthalamic nucleus stimulation. Conf Proc IEEE Eng Med Biol Soc. 2009; 2009:3306–3309. [PubMed: 19964299]
28. Ortiz AN, Kurth BJ, Osterhaus GL, Johnson MA. Dysregulation of intracellular dopamine stores revealed in the R6/2 mouse striatum. J Neurochem. 2010; 112:755–761. [PubMed: 19929911]
29. Yorgason JT, España RA, Jones SR. Demon voltammetry and analysis software: analysis of cocaine-induced alterations in dopamine signaling using multiple kinetic measures. Journal of neuroscience methods. 2011; 202:158–164. [PubMed: 21392532]
30. Fukuda A, Czurko A, Hida H, Muramatsu K, Lenard L, Nishino H. Appearance of deteriorated neurons on regionally different time tables in rat brain thin slices maintained in physiological condition. Neurosci Lett. 1995; 184:13–16. [PubMed: 7739796]
31. Buskila Y, Breen PP, Tapson J, van Schaik A, Barton M, Morley JW. Extending the viability of acute brain slices. Sci Rep. 2014; 4:5309. [PubMed: 24930889]
32. Richerson GB, Messer C. Effect of composition of experimental solutions on neuronal survival during rat brain slicing. Exp Neurol. 1995; 131:133–143. [PubMed: 7895807]
33. Ullrich C, Daschil N, Humpel C. Organotypic vibrosections: novel whole sagittal brain cultures. J Neurosci Methods. 2011; 201:131–141. [PubMed: 21835204]
34. Ferris MJ, Calipari ES, Yorgason JT, Jones SR. Examining the complex regulation and drug-induced plasticity of dopamine release and uptake using voltammetry in brain slices. ACS chemical neuroscience. 2013; 4:693–703. %@ 1948–7193. [PubMed: 23581570]
35. Shang, C-f, Li, X-q, Yin, C., Liu, B., Wang, Y-f, Zhou, Z., Du, J-l. Amperometric Monitoring of Sensory-Evoked Dopamine Release in Awake Larval Zebrafish. The Journal of Neuroscience. 2015; 35:15291–15294. [PubMed: 26586817]
36. Rink E, Wullimann MF. The teleostean (zebrafish) dopaminergic system ascending to the subpallium (striatum) is located in the basal diencephalon (posterior tuberculum). Brain Res. 2001; 889:316–330. [PubMed: 11166725]
37. Rink E, Wullimann MF. Connections of the ventral telencephalon (subpallium) in the zebrafish (Danio rerio). Brain Res. 2004; 1011:206–220. [PubMed: 15157807]
38. Tay TL, Ronneberger O, Ryu S, Nitschke R, Driever W. Comprehensive catecholaminergic projectome analysis reveals single-neuron integration of zebrafish ascending and descending dopaminergic systems. Nat Commun. 2011; 2:1–12. 12.
39. Kile BM, Walsh PL, McElligott ZA, Bucher ES, Guillot TS, Salahpour A, Caron MG, Wightman RM. Optimizing the Temporal Resolution of Fast-Scan Cyclic Voltammetry. ACS Chem Neurosci. 2012; 3:285–292. [PubMed: 22708011]
40. Cragg SJ, Greenfield SA. Differential autoreceptor control of somatodendritic and axon terminal dopamine release in substantia nigra, ventral tegmental area, and striatum. J Neurosci. 1997; 17:5738–5746. [PubMed: 9221772]

41. Garris PA, Christensen JRC, Rebec GV, Wightman RM. Real-time measurement of electrically evoked extracellular dopamine in the striatum of freely moving rats. J Neurochem. 1997; 68:152–161. [PubMed: 8978721]
42. Cooper, JR., Bloom, FE., Roth, RH. The biochemical basis of neuropharmacology. Oxford University Press; 2003.
43. Jones SR, Gainetdinov RR, Jaber M, Giros B, Wightman RM, Caron MG. Profound neuronal plasticity in response to inactivation of the dopamine transporter. Proceedings of the National Academy of Sciences. 1998; 95:4029–4034.
44. Jones SR, Joseph JD, Barak LS, Caron MG, Wightman RM. Dopamine neuronal transport kinetics and effects of amphetamine. Journal of neurochemistry. 1999; 73:2406–2414. [PubMed: 10582600]
45. Richelson E. Antidepressants: pharmacology and clinical use. Treatments of psychiatric disorders. 1989; 3:1773–1786.
46. Fuller RW, Wong DT, Robertson DW. Fluoxetine, a selective inhibitor of serotonin uptake. Medicinal research reviews. 1991; 11:17–34. [PubMed: 1994152]
47. Hashemi P, Dankoski EC, Lama R, Wood KM, Takmakov P, Wightman RM. Brain dopamine and serotonin differ in regulation and its consequences. Proceedings of the National Academy of Sciences of the United States of America. 2012; 109:11510–11515. [PubMed: 22778401]
48. Lengyel K, Pieschl R, Strong T, Molski T, Mattson G, Lodge NJ, Li Y-W. Ex vivo assessment of binding site occupancy of monoamine reuptake inhibitors: methodology and biological significance. Neuropharmacology. 2008; 55:63–70. [PubMed: 18538356]
49. Roubert C, Sagné C, Kapsimali M, Vernier P, Bourrat F, Giros B. A Na+/Cl−-dependent transporter for catecholamines, identified as a norepinephrine transporter, is expressed in the brain of the teleost fish medaka (Oryzias latipes). Molecular pharmacology. 2001; 60:462–473. [PubMed: 11502876]
50. Jones SR, Gainetdinov RR, Wightman RM, Caron MG. Mechanisms of amphetamine action revealed in mice lacking the dopamine transporter. Journal of Neuroscience. 1998; 18:1979–1986. [PubMed: 9482784]
51. Kastenhuber E, Kratochwil CF, Ryu S, Schweitzer J, Driever W. Genetic dissection of dopaminergic and noradrenergic contributions to catecholaminergic tracts in early larval zebrafish. Journal of Comparative Neurology. 2010; 518:439–458. [PubMed: 20017210]
52. Shang CF, Li XQ, Yin C, Liu B, Wang YF, Zhou Z, Du JL. Amperometric Monitoring of Sensory-Evoked Dopamine Release in Awake Larval Zebrafish. The Journal of neuroscience : the official journal of the Society for Neuroscience. 2015; 35:15291–15294. [PubMed: 26586817]
53. Boehmler W, Obrecht-Pflumio S, Canfield V, Thisse C, Thisse B, Levenson R. Evolution and expression of D2 and D3 dopamine receptor genes in zebrafish. Developmental dynamics. 2004; 230:481–493. [PubMed: 15188433]
54. Ford CP. The role of D2-autoreceptors in regulating dopamine neuron activity and transmission. Neuroscience. 2014; 282:13–22. [PubMed: 24463000]
55. Walters SH, Robbins EM, Michael AC. Modeling the kinetic diversity of dopamine in the dorsal striatum. ACS Chem Neurosci. 2015; 6:1468–1475. [PubMed: 26083009]
56. Taylor IM, Ilitchev AI, Michael AC. Restricted diffusion of dopamine in the rat dorsal striatum. ACS chemical neuroscience. 2013; 4:870–878. [PubMed: 23600442]
57. Walters SH, Taylor IM, Shu Z, Michael AC. A novel restricted diffusion model of evoked dopamine. ACS chemical neuroscience. 2014; 5:776–783. [PubMed: 24983330]
58. Hoffman AF, Spivak CE, Lupica CR. Enhanced Dopamine Release by Dopamine Transport Inhibitors Described by a Restricted Diffusion Model and Fast-Scan Cyclic Voltammetry. ACS chemical neuroscience. 2016
59. Wightman R, Amatorh C, Engstrom R, Hale P, Kristensen E, Kuhr W, May L. Real-time characterization of dopamine overflow and uptake in the rat striatum. Neuroscience. 1988; 25:513–523. [PubMed: 3399057]
60. Johnson MA, Rajan V, Miller CE, Wightman RM. Dopamine release is severely compromised in the R6/2 mouse model of Huntington's disease. Journal of neurochemistry. 2006; 97:737–746. [PubMed: 16573654]

61. Peters JL, Michael AC. Modeling voltammetry and microdialysis of striatal extracellular dopamine: the impact of dopamine uptake on extraction and recovery ratios. Journal of neurochemistry. 1998; 70:594–603. [PubMed: 9453553]

62. Peters JL, Michael AC. Changes in the kinetics of dopamine release and uptake have differential effects on the spatial distribution of extracellular dopamine concentration in rat striatum. Journal of neurochemistry. 2000; 74:1563–1573. [PubMed: 10737613]

63. Mitch Taylor I, Jaquins-Gerstl A, Sesack SR, Michael AC. Domain-dependent effects of DAT inhibition in the rat dorsal striatum. Journal of neurochemistry. 2012; 122:283–294. [PubMed: 22548305]

64. Hrabětová S, Nicholson C. Contribution of dead-space microdomains to tortuosity of brain extracellular space. Neurochemistry international. 2004; 45:467–477. [PubMed: 15186912]

65. Hrabětová S, Masri D, Tao L, Xiao F, Nicholson C. Calcium diffusion enhanced after cleavage of negatively charged components of brain extracellular matrix by chondroitinase ABC. The Journal of physiology. 2009; 587:4029–4049. [PubMed: 19546165]

66. Wu Q, Reith MEA, Wightman RM, Kawagoe KT, Garris PA. Determination of release and uptake parameters from electrically evoked dopamine dynamics measured by real-time voltammetry. J Neurosci Methods. 2001; 112:119–133. [PubMed: 11716947]

67. Kraft J, Osterhaus G, Ortiz A, Garris P, Johnson M. In vivo dopamine release and uptake impairments in rats treated with 3-nitropropionic acid. Neuroscience. 2009; 161:940–949. [PubMed: 19362126]

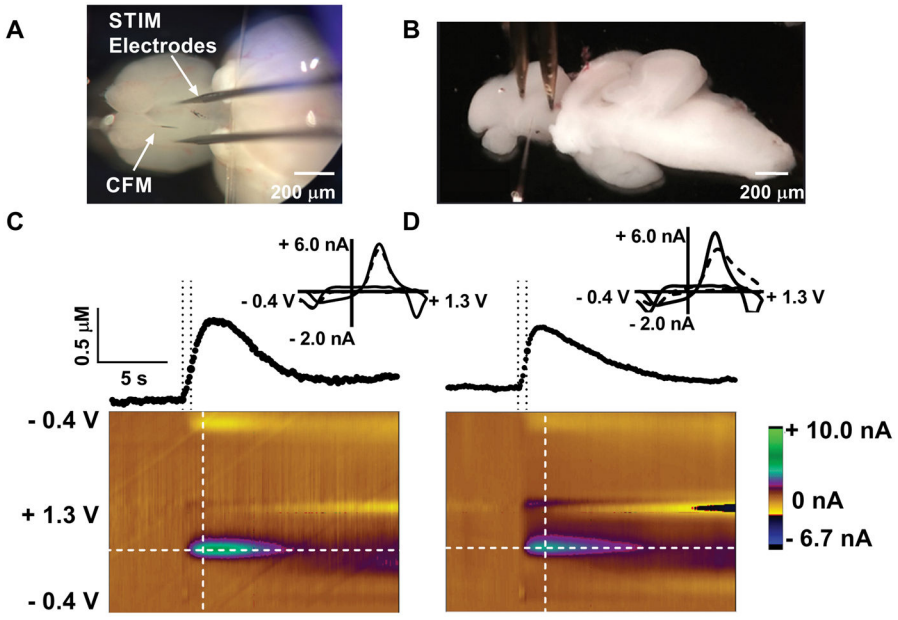

Figure 1.

Electrically-evoked dopamine release in zebrafish whole brain and sagittal brain slices. Images of a whole brain (A) and a sagittal slice (B) indicate the placement of carbon-fiber and stimulus electrodes in the ventral telencephalon. Representative data of evoked dopamine release in a whole brain (C) and a sagittal brain slice (D) are shown. For C and D, the stimulated release plots (top) were sampled at the horizontal white dashed lines and the cyclic voltammograms (insets) were sampled at the vertical white dashed lines of the color plots. The stimulation times are indicated on the release plots by the time between the dashed lines. The CVs (dotted lines) are overlaid with sample voltammograms from the flow cell represented by the solid line.

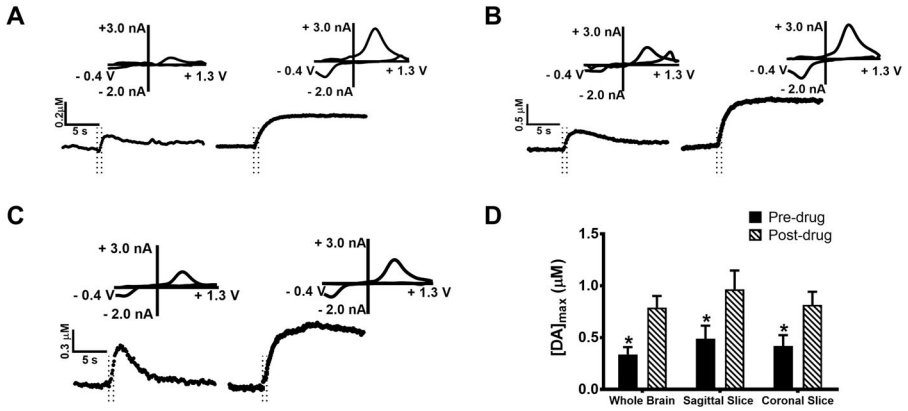

Figure 2.

The effect of uptake inhibition on dopamine overflow in whole brain (A), sagittal slices (B), and coronal slices (C). Dopamine release was measured before and after 10 μM nomifensine was administered to each preparation. The current versus time profiles show that dopamine uptake was diminished. Dopamine overflow after nomifensine addition was significantly increased in whole brain ($p < 0.05$, $n = 4$ brains, t-test), sagittal slices ($p < 0.05$, $n = 5$ slices, t-test) and coronal slices ($p < 0.05$, $n = 4$, t-test) (D). Stimulation time is indicated on the release plots by the time between the dashed lines.

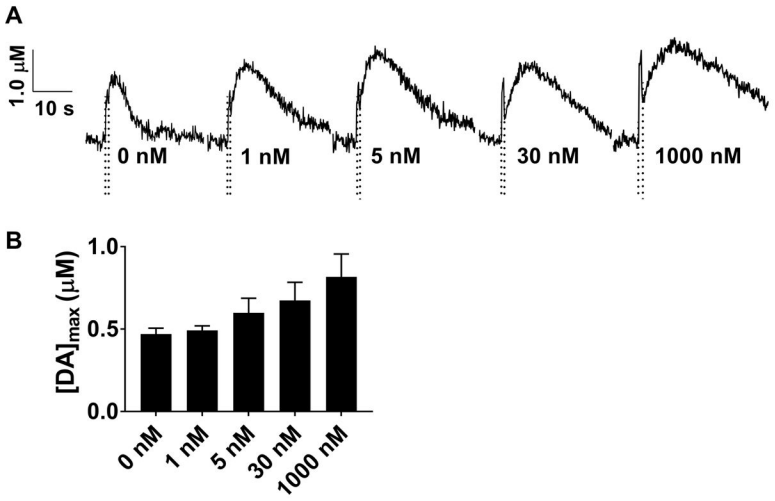

Figure 3.

The effect of lower concentrations of nomifensine on dopamine overflow in the whole brain. (A) Representative stimulated release plots are shown for different concentrations (0, 1, 5, 30, 1000 nM) of nomifensine perfused over whole brain preparations. Stimulation time is indicated on the release plots by the time between the dashed lines. (B) Effect of nomifensine on dopamine overflow in whole brain. No overall effect on $[DA]_{max}$ was observed ($p=0.11$, one-way ANOVA, $n=3$ brains).

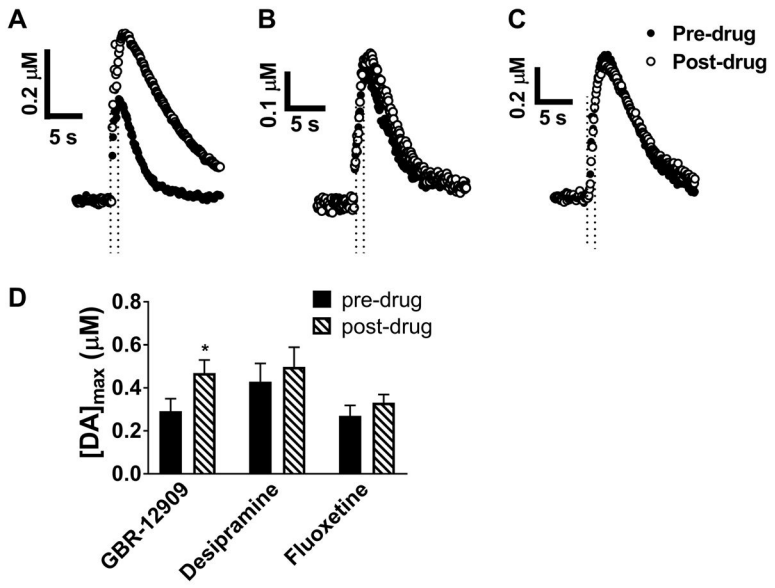

Figure 4.

The effects of dopamine transporter (DAT), serotonin transporter (SERT), and norepinephrine transporter (NET) inhibition on dopamine release in whole brains. Representative stimulated release plots were obtained before and after perfusion with 10 μM GBR-12909 (A), desipramine (B), and fluoxetine (C). Comparisons of $[DA]_{max}$ before and after perfusion are shown in (D). Treatment with GBR-12909 resulted in a significant increase in $[DA]_{max}$ (*$p < 0.05$, t-test, n=5 brains). No significant changes in release were noted after treatment with desipramine or fluoxetine ($p= 0.595$ and 0.347 for desipramine and fluoxetine, respectively, t-tests, n=5 brains). Stimulation time is indicated on the release plots by the time between the dashed lines.

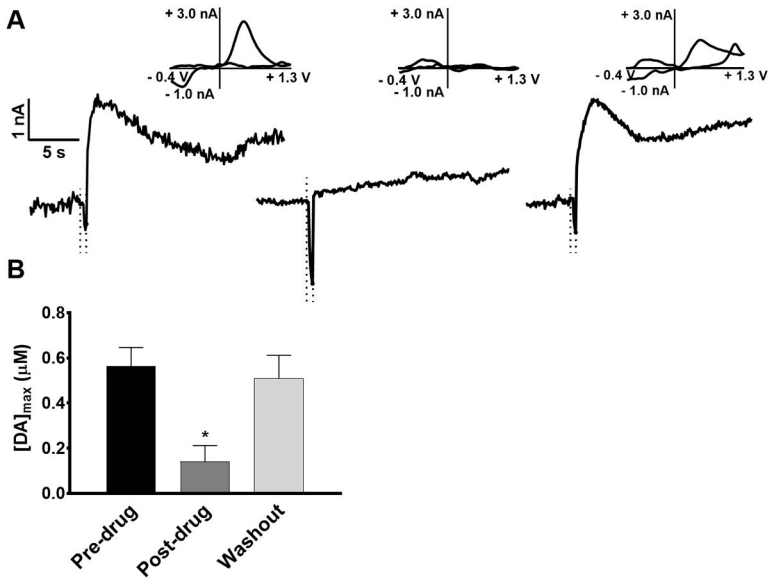

Figure 5.

The effect of dopamine synthesis inhibition on stimulated release. (A) Representative data of stimulated dopamine release before (left) and after (center) administration of 50 μM αMPT. Dopamine release reappeared after a 1-hour washout with drug-free buffer solution in the same recording session (right). Cyclic voltammograms for each step (inserts) confirm the release of dopamine. The sharp dip in current prior to the faradaic peak is an artifact occurring due to stimulation. (B) Evoked dopamine release, measured after 2 hours of treatment with αMPT was significantly decreased ($p < 0.01$, one way ANOVA, tukey post hoc test, *$p < 0.05$, n=5 brains). Dopamine release after washout was not significantly different from the pre-drug measurement ($p = 0.40$, one way ANOVA, n=5). Stimulation time is indicated by the dotted lines.

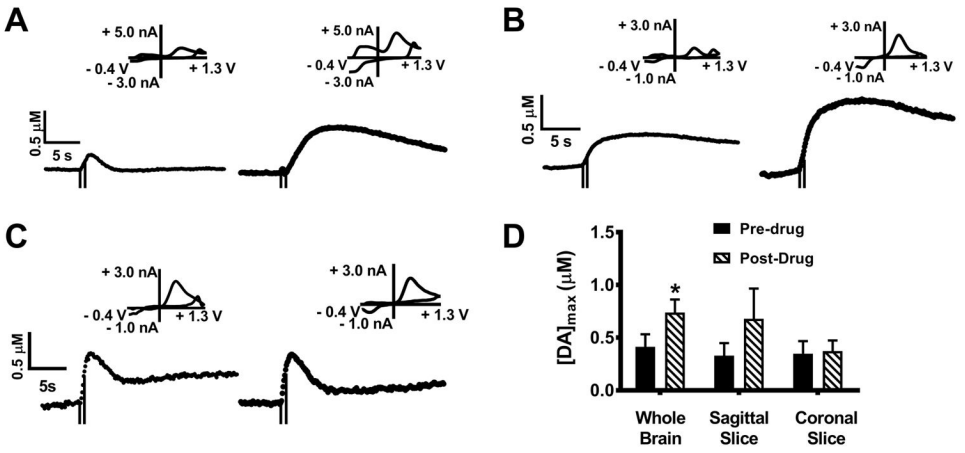

Figure 6.

Effect of sulpiride treatment on dopamine release. Evoked dopamine release measured in (A) whole brain, (B) sagittal slice, and (C) coronal slice before and after treatment with 10 µM sulpiride. (D) Dopamine release significantly increased in whole brains ($p < 0.05$, t-test, n=5), but did not significantly increase in sagittal and coronal slices after drug treatment ($p = 0.13$ and $p = 0.47$, respectively, t-test, n= 5). Stimulation times are indicated by vertical lines on release plots.

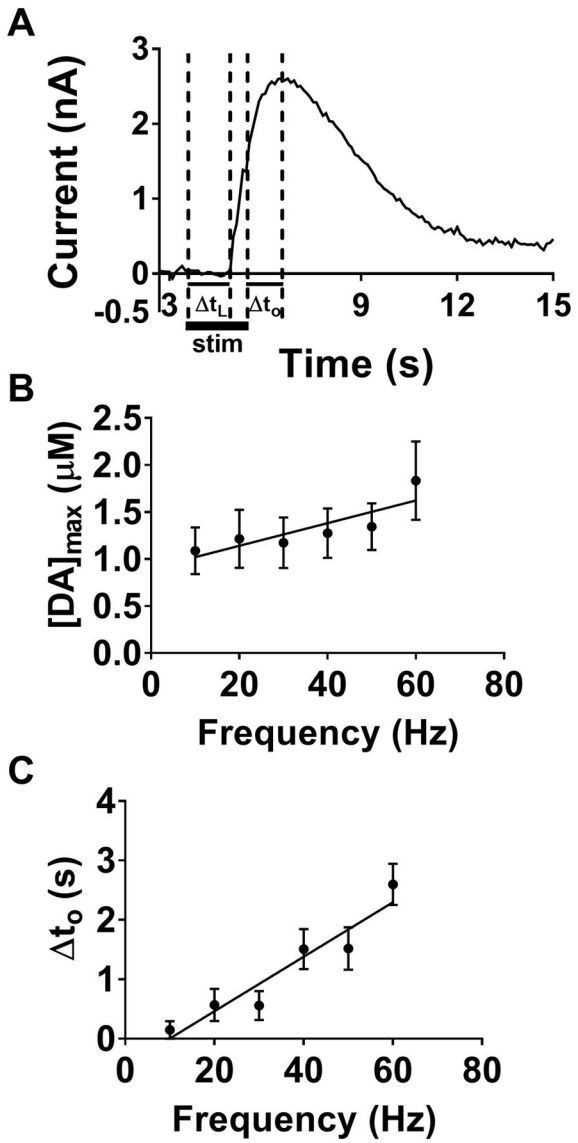

Figure 7.

$[DA]_{max}$, lag time (Δt_L), and overshoot time (Δt_O). The concept of lag and overshoot is illustrated in (A). Lag (Δt_L) is the time after the stimulation begins until dopamine release is observed. Overshoot (Δt_O) is the time after the stimulation ends until $[DA]_{max}$ is reached. The duration of stimulation is indicated by the thick line below the release plot. The effect of increasing stimulation frequency on $[DA]_{max}$ (B) and Δt_O (C) is shown. Linear regression analysis showed that both parameters increased with respect to frequency with non-zero slopes (B, slope $\neq 0$, $p < 0.05$, $R^2 = 0.725$; C, slope $\neq 0$, $p < 0.005$, $R^2 = 0.908$ respectively).

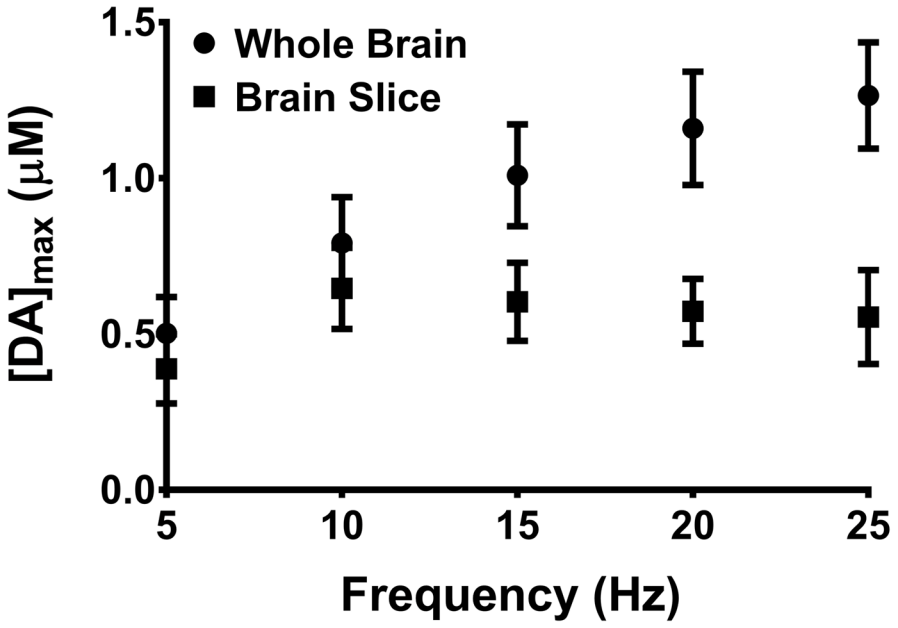

Figure 8.

Effect of stimulation frequency on dopamine release. The stimulation frequency was increased while stimulation pulses and width were kept constant (120 pulses, 4 ms pulse duration). Evoked dopamine release was measured both in whole brain and sagittal slices. A linear regression was done for both preparations. The whole brain data had a significant non-zero slope ($R^2 = 0.96$, $p = 0.003$) while the slice preparation was found to have no significant slope ($R^2 = 0.17$, $p = 0.49$).